forests

MDPI

Article

Single-Sided Microwave Near-Field Scanning of Pine Wood Lumber for Defect Detection

Mohamed Radwan, David V. Thiel and Hugo G. Espinosa *

School of Engineering and Built Environment, Nathan Campus, Griffith University, Brisbane City, QLD 4111, Australia; mohamed.radwan@griffithuni.edu.au (M.R.); d.thiel@griffith.edu.au (D.V.T.)
* Correspondence: h.espinosa@griffith.edu.au; Tel.: +61-7-3735-8432

Abstract: Defects and cracks in dried natural timber (relative permittivity 2–5) may cause structural weakness and enhanced warping in structural beams. For a pine wood beam (1200 mm × 70 mm × 70 mm), microwave reflection (S_{11}) and transmission (S_{21}) measurements using a cavity-backed slot antenna on the wood surface showed the variations caused by imperfections and defects in the wood. Reflection measurements at 4.4 GHz increased (>5 dB) above a major knot evident on the wood surface when the E-field was parallel to the wood grain. Similar results were observed for air cavities, independent of depth from the wood surface. The presence of a metal bolt in an air hole increased S_{11} by 2 dB. In comparison, transmission measurements (S_{21}) were increased by 6 dB for a metal screw centered in the cavity. A kiln-dried pine wood sample was saturated with water to increase its moisture content from 17% to 138%. Both parallel and perpendicular E-field measurements showed a difference of more than 15 dB above an open saw-cut slot in the water-saturated beam. The insertion of a brass plate in the open slot created a 7 dB rise in the S_{11} measurement ($p < 0.0003$), while there was no significant variation for perpendicular orientation. By measuring the reflection coefficient, it was possible to detect the location of a crack through a change in its magnitude without a noticeable change (<0.01 GHz) in resonant frequency. These microwave measurements offer a simple, single-frequency non-destructive testing method of structural timber in situ, when one or more plane faces are accessible for direct antenna contact.

Keywords: non-destructive testing; near-field; cavity-backed slot antenna; microwaves

check for updates

Citation: Radwan, M.; Thiel, D.V.; Espinosa, H.G. Single-Sided Microwave Near-Field Scanning of Pine Wood Lumber for Defect Detection. *Forests* **2021**, *12*, 1486. https://doi.org/10.3390/f12111486

Academic Editor: Ian D. Hartley

Received: 16 August 2021
Accepted: 26 October 2021
Published: 29 October 2021

Publisher's Note: MDPI stays neutral with regard to jurisdictional claims in published maps and institutional affiliations.

Copyright: © 2021 by the authors. Licensee MDPI, Basel, Switzerland. This article is an open access article distributed under the terms and conditions of the Creative Commons Attribution (CC BY) license (https://creativecommons.org/licenses/by/4.0/).

1. Introduction

Sustainability is an important aspect of structural engineering. As wood is a naturally occurring material, timber beams in multistory buildings have become increasingly desirable as a renewable material of choice [1–4]. With greater flexibility than steel and concrete, and a higher strength-to-mass ratio, timber constructions offer many advantages in both transport and construction costs, as well as durability [5,6], even though timber does suffer from points of weakness related to knots, grain anisotropy, and flammability.

Methods for measuring the strength characteristics of wood in situ (i.e., after the construction of a building) are limited. There are difficult and unresolvable issues related to non-destructive testing (NDT) techniques such as acoustics and ultrasonics. Acoustic wave velocity (AWV) was used as an early selection method for structural boards of Eucalyptus timber [7]. Near-infrared spectroscopy was utilized to detect the presence of three different oils in Cryptomeria japonica and Chamaecyparis obtuse wood samples that were used in Japanese construction [8]. The possibility of using near-field microwave measurements with a single antenna is one option that has yet to be explored in significant detail. Thus, the research question addressed in this paper is:

Can near-field microwave measurements provide information about the uniformity of natural timber beams in situ?

Material evaluation has been achieved through a number of physical methods. Non-destructive testing involves the identification and characterization of the damage on the surface and within the interior of the material, without weakening the structure or removing

samples [9]. Non-destructive testing technologies can be categorized as contact and non-contact methods. Contact methods require good contact between the sensor and the material. Topographic imaging using a stress wave detected and visualized defect areas inside trees [10]. A tomographic imaging algorithm (IABLE) with a velocity error correction mechanism was developed for the high-resolution evaluation of wood [11]. Non-contact methods can be conducted remotely with an air gap between the sensors and the material under test.

Most electromagnetic detection techniques require the simultaneous measurement of the transmission and reflection of radio waves. This paper describes a contact electromagnetic method for NDT, in which the effect of the wood beam on the input impedance of an antenna at microwave frequencies is determined. Variations in the microwave transmission data through the wood were used as a verification-sensing method for internal nonuniformities.

Microwave signals can penetrate lossy media and induce electric currents inside the material. When the current path is deformed by anomalies in the wood, the input impedance of the antenna is impacted. This technique has many advantages, including providing sensor hardware simplicity, low power consumption, and high reliability of detection [10]; more importantly, access to only one flat face of the beam is required.

Microwaves and other methods have been used to measure the permittivity of timber with three main objectives: (a) to assess the biomass for possible power generation, (b) to understand the fire safety of wood, and (c) to verify wood quality before manufacturing use [8,9]. Another use of these measurements is the non-destructive assessment of wooden artefacts in which woodworm damage may be hidden from the surface [12]. Ramasamy and Moghtaden [8] used wood samples placed in a short-circuit rectangular waveguide and deduced the anisotropic properties, whereas Olmi et al. [13] reported an open-circuit coaxial transmission line placed against a surface so that only an averaged isotropic measurement was possible [14]. The field penetration of the coaxial probe in wood was calculated to be approximately 10 mm at 2–3 GHz. In these cases, both the moisture content (up to 30%) and temperature had a significant effect on the relative permittivity measurements. In most wooden structures, the wood is cured, and the moisture content is very low, resulting in small values for conductivity and the loss tangent.

In this experiment, the near-field of a cavity-backed slot antenna was used in two modalities: (a) The primary method was to measure the antenna input impedance using S_{11}, and (b) the follow-up method used the transmission power between two antennas on different faces of the wood beam. The maximum sensitivity of the antenna impedance is achieved when the S_{11} value is minimum—the resonant frequency—and changes in S_{11} reflect changes in the wood close to the antenna aperture. This technique has the advantages of being non-destructive and polarization-dependent, so the wood anisotropy can be determined. The proximity of an electromagnetic sensor to wood with a rough surface was reported by Olmi et al. [14]. They used a coaxial probe for the permittivity measurements and observed that the surface roughness had a relatively small effect on the measurements. The wood sample used in the present study was kiln-dried, dressed pine timber beam, so the antenna could be readily placed on flat surfaces.

Electromangetic Theory

Electromagnetic (EM) waves propagating through different media have an attenuation and phase velocity dependent on the relative permittivity and conductivity of the material [15]. Antennas are used to convert electric current to EM waves and to convert EM waves to an electric current. When the conversion is most efficient, the reflection coefficient S_{11} is minimum, and the antenna is said to be resonant. At this frequency, the impedance of the transmission feed line is matched to the antenna in contact with material having a different intrinsic impedance. There is maximum power transfer into the material at the resonant frequency.

The complex permittivity (ε_c) of pine wood can be written as:

$$\varepsilon_c = \varepsilon' - j\varepsilon'' \quad (1)$$

where $\varepsilon = \varepsilon'$ and $\varepsilon'' = \sigma/\omega$.

Here, σ and ε' are the conductivity and electric permittivity of the wood, respectively. The angular frequency of the radiation is ω, ε_r is the relative permittivity, and ε_0 is the permittivity of free space:

$$\frac{\varepsilon''}{\varepsilon'} = \frac{\sigma}{\omega \varepsilon_r \varepsilon_o} \tag{2}$$

If a plane EM wave is travelling at the boundary of two materials (i.e., air and wood) with different permittivity, permeability, and impedance, part of the energy will be reflected at that boundary. Because both materials have no magnetic properties, the reflection of the plane EM wave is due to the impedance discontinuity. The reflection and transmission coefficients (S_{11}) and (S_{21}) can then be defined as:

$$S_{11} = \frac{E_{re}}{E_{in}} = \frac{\sqrt{\varepsilon_{r1}} - \sqrt{\varepsilon_{r2}}}{\sqrt{\varepsilon_{r1}} + \sqrt{\varepsilon_{r2}}} \tag{3}$$

$$S_{21} = \frac{E_{tr}}{E_{in}} \tag{4}$$

where E_{in}, E_{re}, E_{tr} are the incident, reflected, and transmitted electric fields, respectively, and ε_{r1} and ε_{r2} are the relative permittivity of the air and wood, respectively.

From antenna theory, the reflection coefficient or return loss of an antenna quantifies how much power is reflected back along the feed transmission line from the antenna terminals. The measurement of S_{11} can therefore indicate a change in the electromagnetic characteristics of the material close to the antenna. In this study, the return loss from a cavity-backed resonant slot antenna lightly pressed onto the wood surface was used [16,17]. The advantage of this antenna is that it can be pressed against the material under test without impacting the measurement. If the impedance in the material changes in the immediate vicinity of the aperture, these changes can be identified in the reactive near-field of the antenna.

S_{11} was measured by moving the antenna along the wood surface and across the region with the cut. The moisture content of the wood was measured using the drying oven method according to Equation (5) in [18]:

$$Moisture\ content\ (\%) = \frac{Initial\ mass - Dry\ mass}{Dry\ mass} \times 100 \tag{5}$$

First, a wood saw was used to cut 20 small ($5 \times 5 \times 5$ mm^3) wood samples. The samples were weighed to determine the initial mass and placed in a well-ventilated oven with the temperature controlled to 101° for 3 h. The dried wood samples were weighed again for the mass calculations. The average moisture content of the dried, dressed wood was 17%. Subsequently, the moisture content of wood was increased by submerging wood samples in water for 24 h and the oven-drying procedure was repeated to calculate the moisture content of wet wood samples. The moisture content percentage increased to 138%.

2. Materials and Methods

2.1. Antenna Characteristics

The antenna used for the reflection measurements was a cavity-backed slot antenna machined from aluminum (overall dimensions: 59 mm × 35 mm × 12 mm) with a resonant slot (30 mm × 13 mm) [19], as shown in Figure 1. The antenna feed was a triangular plate electromagnetically coupled with the slot. The total weight of the antenna was 35.3 g. The antenna feed was connected via a low-loss 50 Ω coaxial cable to a vector network analyzer (Fieldfox N9923A) for the S_{11} measurements. The radiation from the antenna slot was linearly polarized with the electric field (E-field) perpendicular to the slot length and so parallel to the longest dimension of the antenna [20].

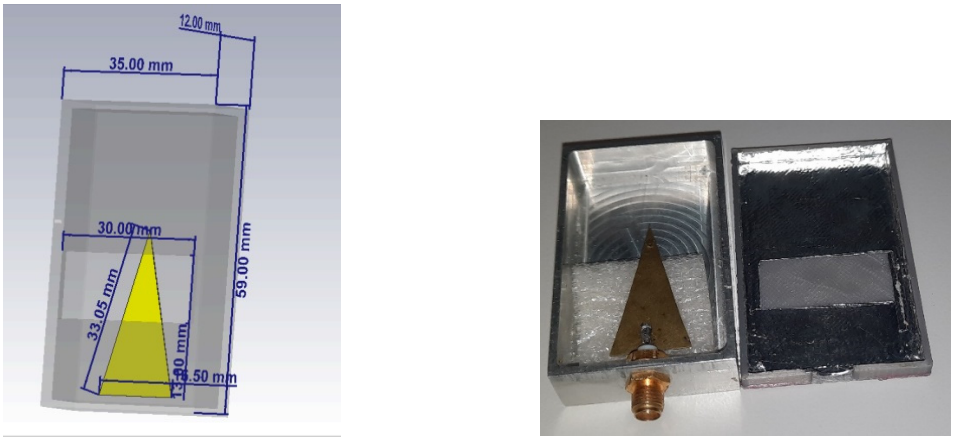

(**a**) (**b**)

Figure 1. Aluminum cavity-backed slot antenna used in reflection measurements: (**a**) antenna dimensions; (**b**) antenna prototype with a 50 Ω SMA connector.

2.2. Wood Measurements

Wood is a natural material with a pronounced grain resulting from yearly growth (annual rings) and so it is both mechanically and electromagnetically anisotropic. Measurements were taken both parallel and perpendicular to the wood grain.

The reflection (S_{11}) measurements were undertaken on pine wood. Wood samples sourced from a local timber merchant were commercially prepared (kiln-dried with a moisture content of 17%) and dressed (i.e., all four sides were smooth). The end face of the pine wood sample showed a section of the annual rings (Figure 2). These wood samples are commonly used in cabinet making and furniture. The measured size and density of the wood samples are given in Table 1 alongside a published value for comparison [21].

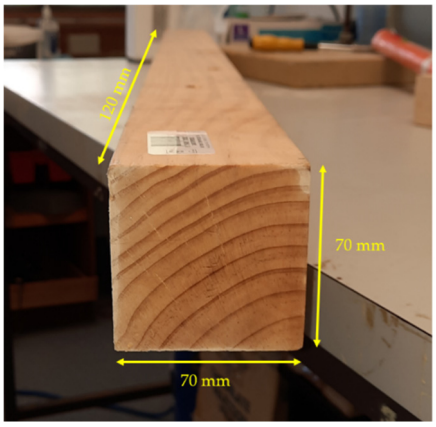

(**a**)

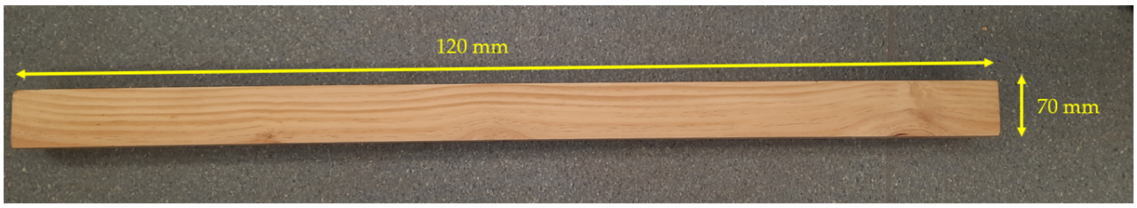

(**b**)

Figure 2. Wood sample: (**a**) the end face of the pine wood sample (70 mm × 70 mm) (Pinus radiata); (**b**) wood sample side view (120 mm × 70 mm).

Table 1. Wood sample characteristics with tabulated density measurements for comparison.

Wood Type (Botanical Name)	Dimensions (Length, Width, Height) (mm)	Weight (kg)	Density (kg/m^3)	Tabulated Density (kg/m^3) [21]
Pine (*Pinus radiata*)	1200 × 70 × 70	2.67	454	545

S_{11} was measured for the E-field directions perpendicular and parallel to the wood grain as shown in Figure 3a,b. When the E-field (+X direction) was parallel to the wood grain (+X direction), the antenna measured parallel polarization. When the E-field (+Y direction) was perpendicular to wood grain (+X direction), the antenna measured perpendicular polarization. At 18 places on the wood with no surface signs of imperfections, parallel and perpendicular polarizations were measured.

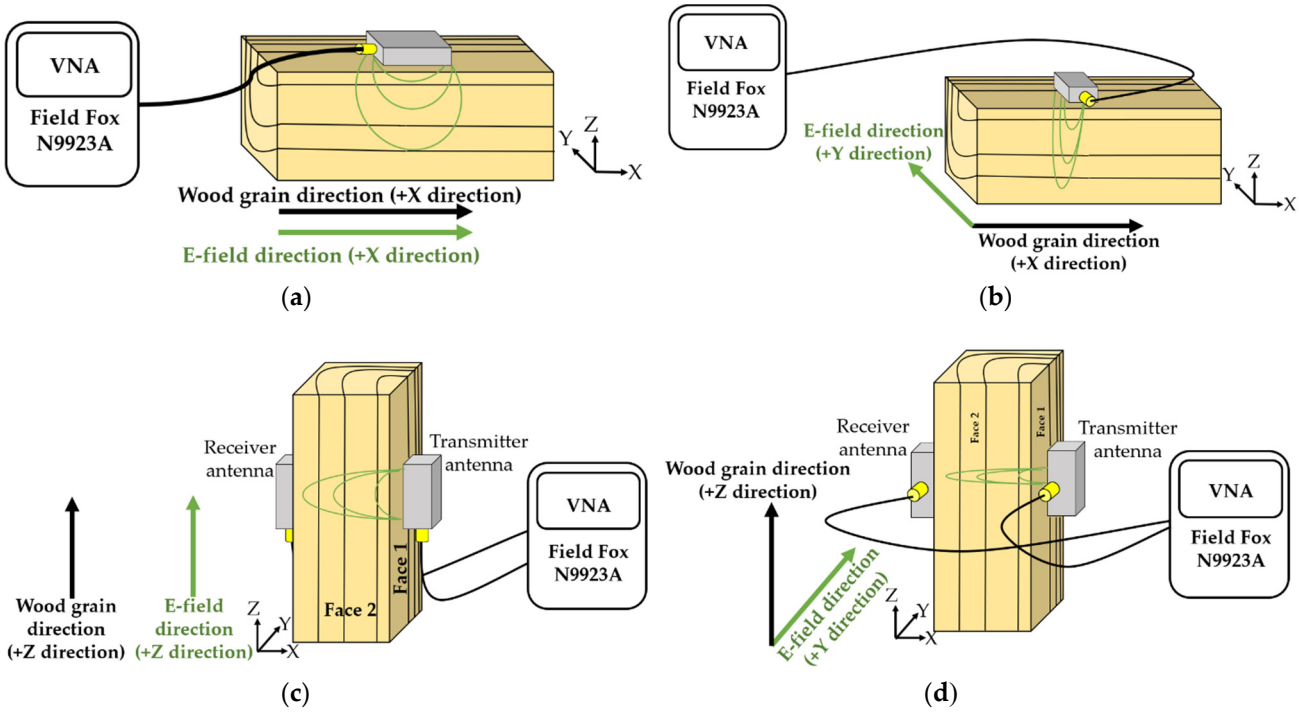

Figure 3. Reflection measurements: (**a**) E-field is parallel to the wood grain; (**b**) E-field is perpendicular to the wood grain. Transmission measurements: (**c**) E-field is parallel to the wood grain; (**d**) E-field is perpendicular to the wood grain.

For the transmission measurements, S_{21} was measured for the E-field directions parallel and perpendicular to the wood annual rings, as shown in Figure 3c,d, respectively. For example, the two antennas were placed on each side of face 1, so the E-field direction (+Z direction) was parallel to the wood grain direction (+Z direction) (Figure 3c). Furthermore, when the two antennas were placed on each side of face 2, the E-field direction (+Y direction) was perpendicular to the wood grain direction (+Z direction).

3. Results

3.1. Antenna Measurements in Air and Wood

The S_{11} of the antenna was measured with the slot in contact with a dry pinewood wood beam. The objective was to assess the variability of the measurements on the S_{11} minimum measurements at the resonant frequency of wood (4.4 GHz, see Figure 4).

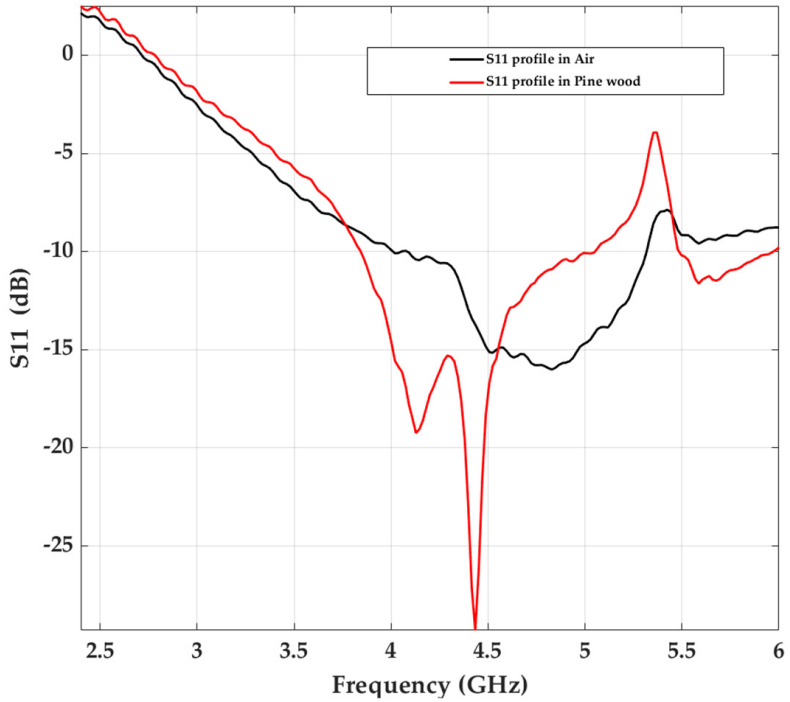

Figure 4. Reflection coefficient (S_{11}) as a function of frequency when the slot was pressed against the pine wood (red line). The black line is the S_{11} for the same antenna measured in air. There is a clear minimum at the resonant frequency of 4.4 GHz.

Measurements were taken at 18 places with no surface signs of imperfections along the 120 cm wood beam. Figure 5 shows that the parallel reflection measurement along wood sample was approximately −17 dB, whereas it was approximately −19 dB for perpendicular measurements. Minor variations are shown for S_{11}, with mean and standard deviations of −17.0 (0.4) dB for parallel and −18.5 (0.2) dB for perpendicular polarization.

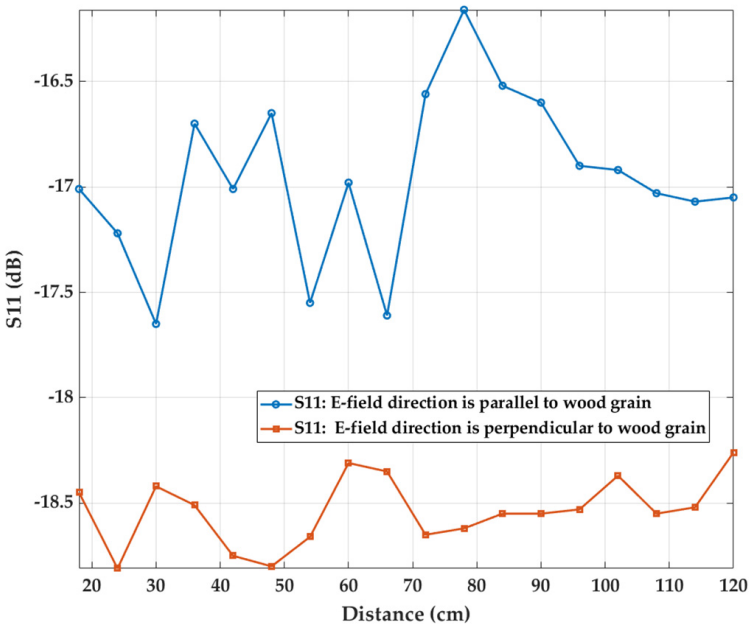

Figure 5. S_{11} reflection measurements along the 120 cm wood sample. The mean and standard deviations in these measurements were −17.0 (0.4) dB for parallel polarization and −18.5 (0.2) dB for perpendicular polarization.

The box-and-whisker plots (Figure 6) for both polarizations showed significant anisotropy at approximately 2.45 GHz. The S_{21} measurements showed no significant anisotropy at 2.45 GHz for the *y* and *z* directions. When the E-field had both perpendicular and parallel polarizations to the wood grain, there was a clear difference (greater than 20 dB) in the received signal for the two polarizations for both faces (Face 1 and Face 2). The explanation for this noticeable difference was the effect of the wood grain annual rings relative to the E field.

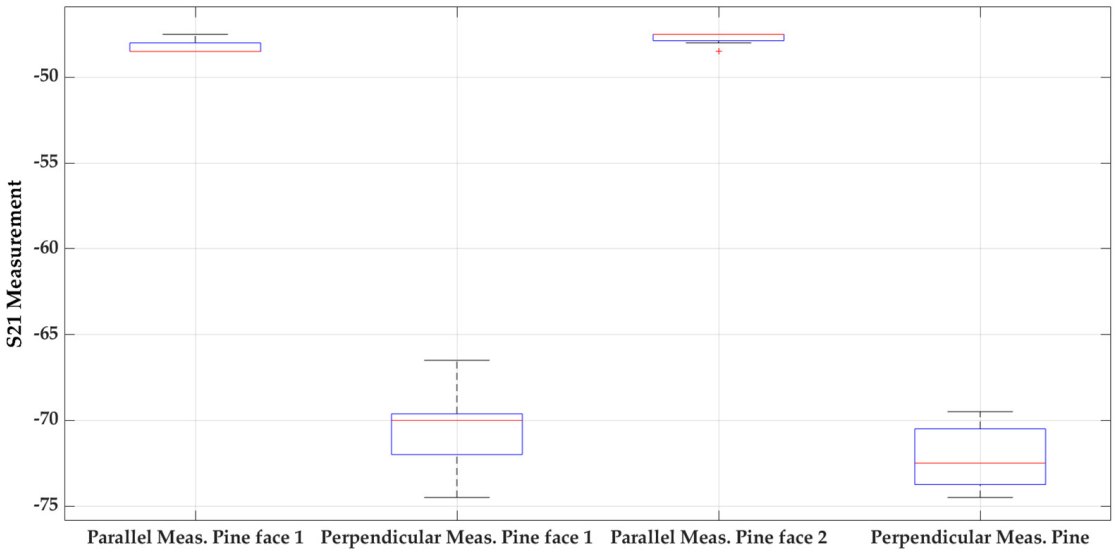

Figure 6. Box-and-whisker plot for the transmission S_{21} between two faces, Face1 and Face 2, for both parallel and perpendicular polarizations. The coefficient of anisotropy for transmission at 2.4 GHz was approximately 26 dB.

3.2. Branch Measurements

Near-field measurements across a wood surface anomaly were performed over a branch mark on a pine wood surface (Figure 7). The antenna was placed on the surface, moved in steps of 2.5 mm across the branch mark, and the S_{11} values were recorded. Both perpendicular and parallel polarizations were used in the measurement process. For parallel measurement, the S_{11} values decreased significantly ($p < 0.0003$) from an average of -20 $\pm$ 2 dB to reach -27 dB at the branch mark position (distance = 0 mm, see Figure 8), while for perpendicular polarization, there was no obvious change in S_{11} across the anomaly.

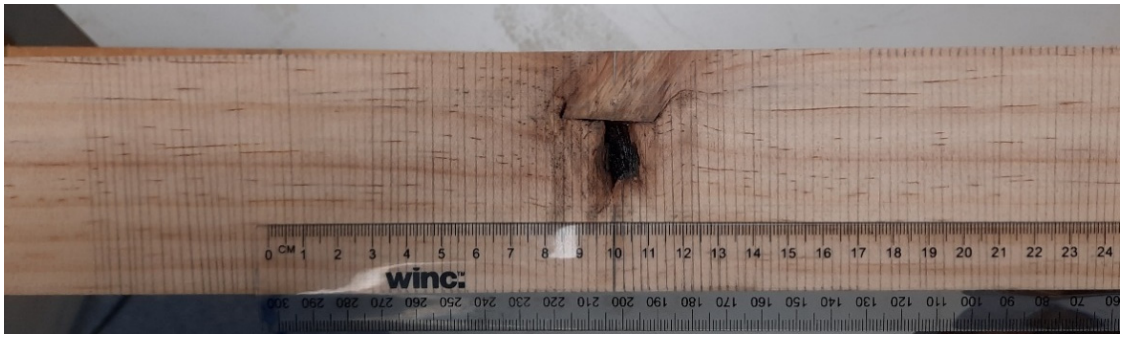

Figure 7. Surface expression of the branch mark on the pine wood surface.

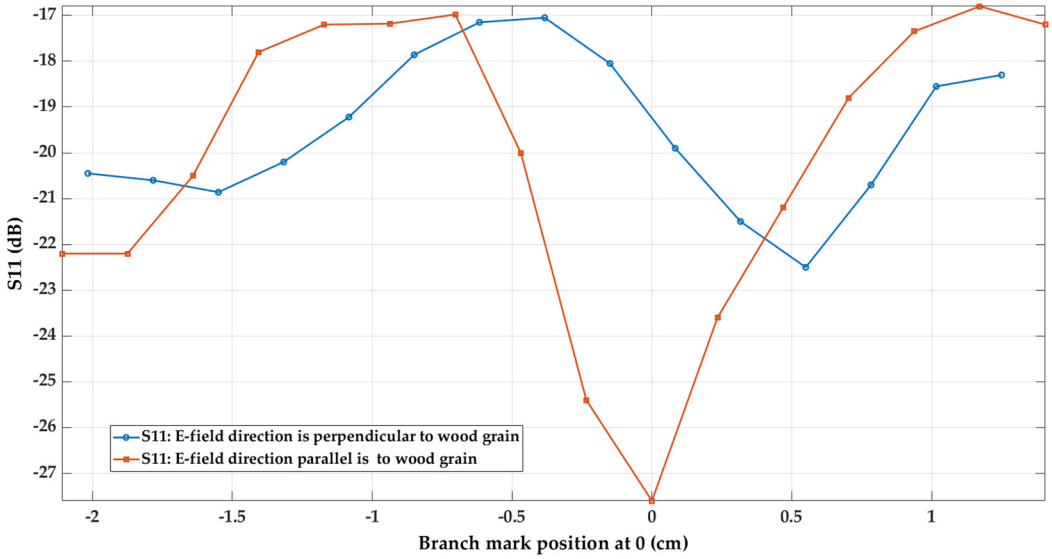

Figure 8. The S_{11} reflection coefficient profile for measurements across the branch mark at 4.4 GHz using both parallel and perpendicular polarizations.

3.3. Cavity Measurements

As parallel measurements showed a more significant effect in the vicinity of the branch anomaly, parallel S_{11} measurements were used in further experiments. Two separated holes (diameter 12.5 mm) were created in the sample. The first hole was 10 mm away from the measurement surface (top of the image) as shown in Figure 9a, and another hole was 30 mm away from the surface (Figure 9b). A steel bolt with the same dimensions as the hole was inserted to observe the effect of a conducting insert inside wooden walls, such as wires and metal screws. In addition, transmission measurements were conducted to observe the effect of the metal inserts in the wood cavities.

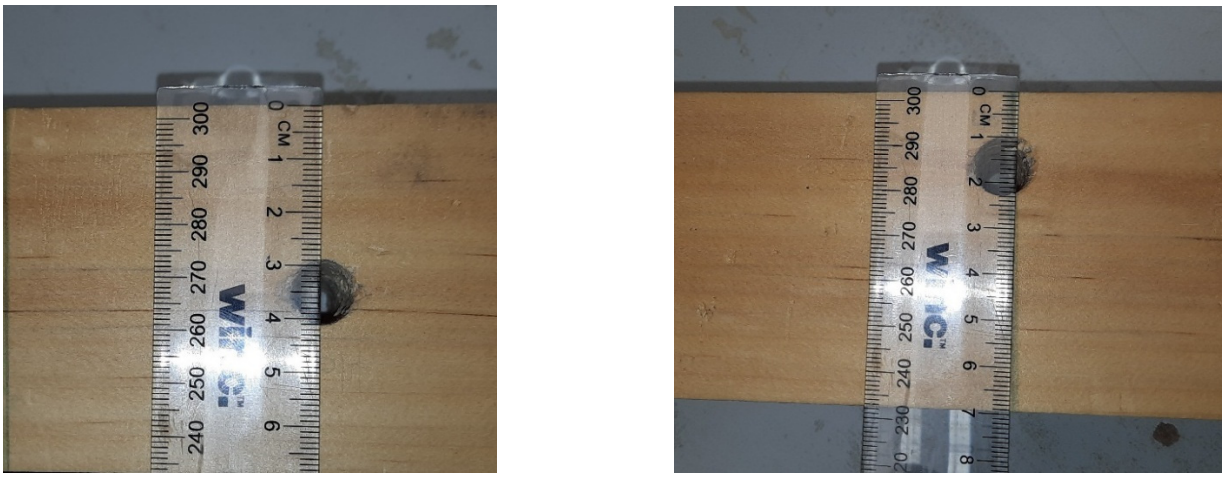

(**a**) (**b**)

Figure 9. Cavities in the wood beam: (**a**) hole is 10 mm from measurement surface; (**b**) hole is 30 mm from measurement surface.

(a) Wood Beam, Hole 30 mm from the Measurement Surface

Figure 10a shows that S_{11} was reduced to −17 dB when the hole was filled with air. When the bolt was inserted, the reflection coefficient reached more than −20 dB. For transmission measurements (Figure 10b), there was no change in S_{21} for an air-filled hole; however, the steel bolt resulted in a significant change to −38 dB immediately above the anomaly at 3.5 cm.

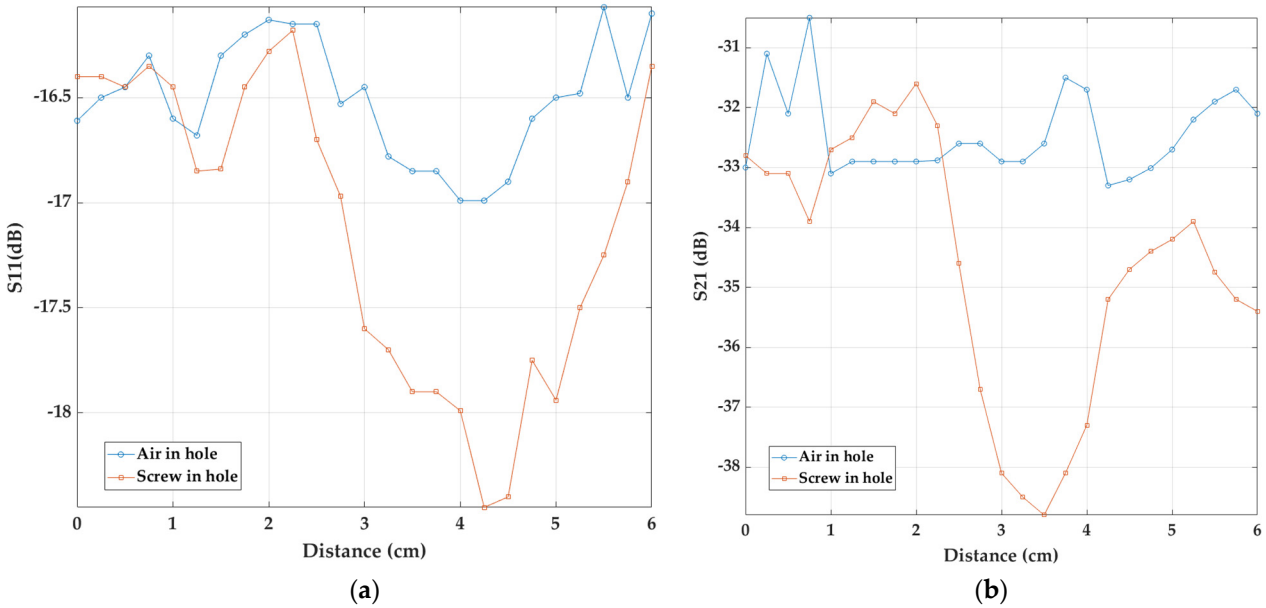

(**a**) (**b**)

Figure 10. S_{11} and S_{21} measurements over the hole at 30 mm from the measurement surface at a distance of 3.5 cm: (**a**) reflection measurements for air-filled hole vs. bolt; (**b**) transmission measurements for the air-filled hole vs. the bolt.

(b) Wood Beam, Hole 10 mm from the Measurement Surface

Figure 11a shows that S_{11} = 17.65 dB increased above the air-filled hole; however, the bolt insert resulted in S_{11} = −17.5 dB, an immense decrease. Air is a very low loss dielectric material, and the hole was in the very near-field E-field region of the antenna. When the hole was filled with a good conductor, S_{11} decreased dramatically. These results were verified by transmission measurements (see Figure 11b), as the S_{21} showed no noticeable change for the air-filled hole, but was sharply reduced to below −48 dB for the conductor-filled hole.

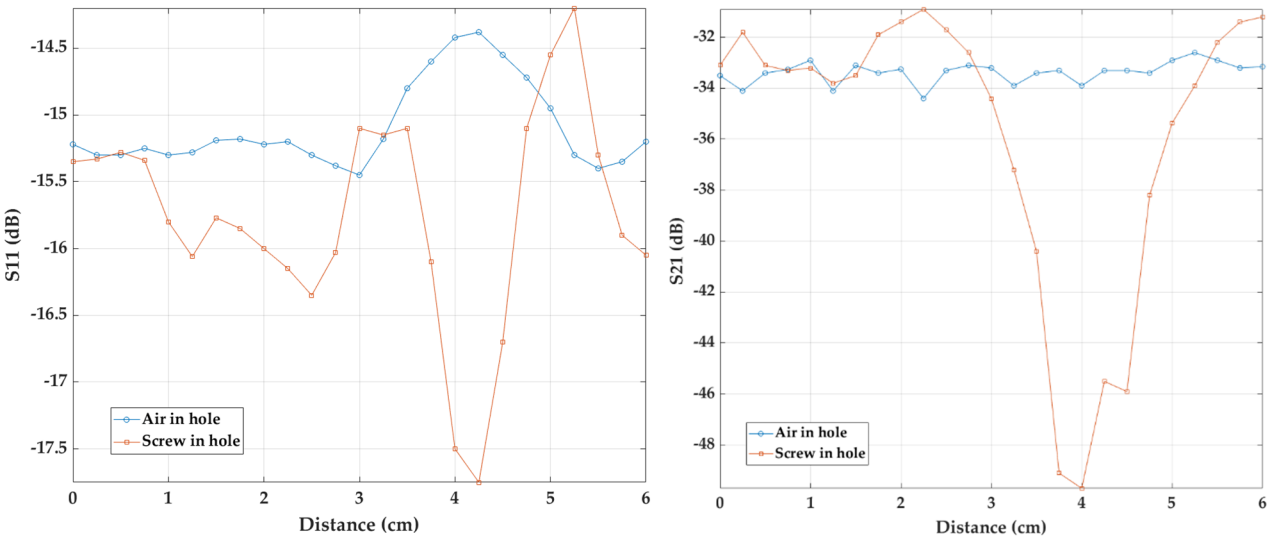

(**a**) (**b**)

Figure 11. The hole was 10 mm from the measurement surface and at 4 cm: (**a**) S_{11} for air-filled hole vs. bolt; (**b**) S_{21} for air-filled hole vs. bolt.

3.4. Moisture Content (MC)

The effect of moisture on the measurements was investigated by comparing dry wood with wet wood across a saw cut. The pine wood sample was partially cut in the

center of its 120 cm length (location number 10 cm). The cut was 2 mm wide and 50 mm deep. S_{11} measurements were made at 4.4 GHz across the cut in two orientations. The first orientation considered the E-field plane direction parallel to the wood grain along the x axis, and perpendicular to the cut (+Y direction) on reverse side (Figure 12a). In the second orientation, the E-field plane was perpendicular to the wood grain along the y direction and parallel to the cut (Figure 12b).

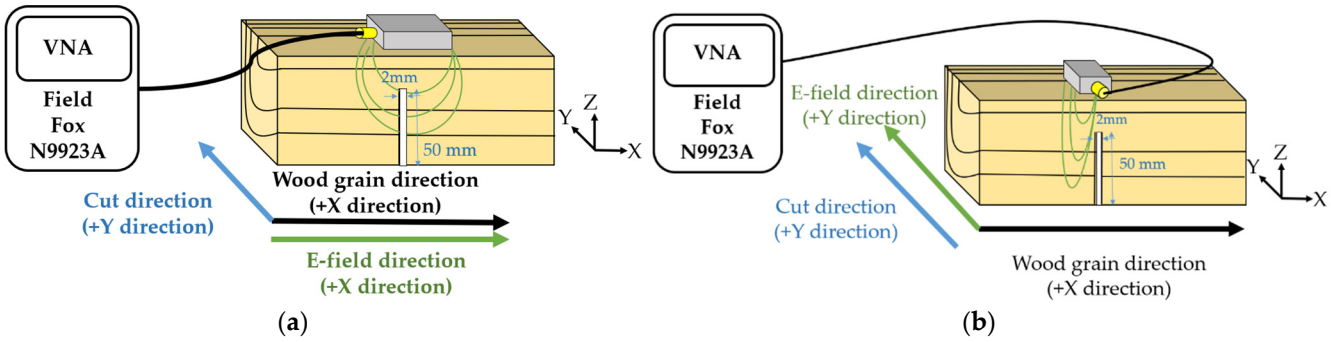

Figure 12. (**a**) E-field parallel to the wood grain and perpendicular to the cut (reverse side); (**b**) E-field perpendicular to the wood grain and parallel to the cut (reverse side).

The microwave measurements showed that immediately above the cut in the wet wood samples (position 0), a reduction of (−10 dB) for the reverse side measurements in the perpendicular orientation to the cut was observed (see Figure 13a). However, reflection measurements peaked at around –30 dB for high-moisture content wood (138%), and the cut had no effect on those measurements, as shown in Figure 13b. In this case, the E-field was aligned parallel to the air-filled cut and there were no variations in reflection coefficient measurements around it.

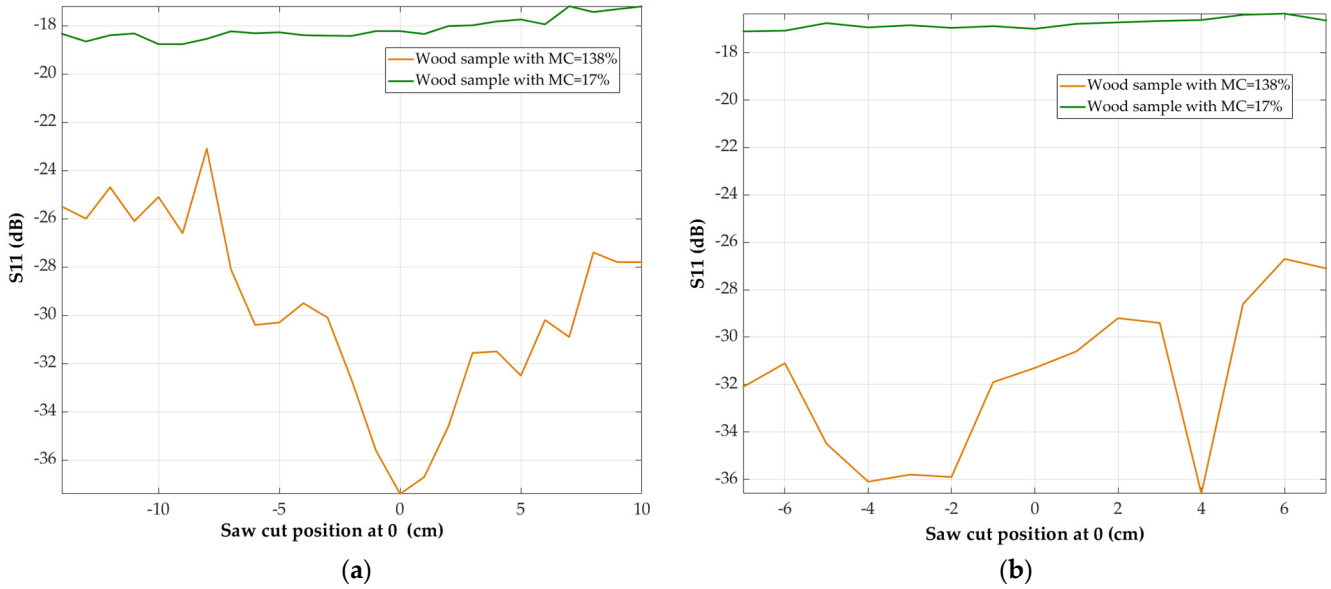

Figure 13. S_{11} measurements for wet and dry wood samples above the saw cut: (**a**) E-field parallel to the wood grain and perpendicular to the cut (reverse side); (**b**) E-field perpendicular to the wood grain and parallel to the cut (reverse side).

During these experiments, no change (<2 dB) in the S_{11} measurements was observed when objects were located immediately below the measurement position. This indicated that the sensitivity of the measurement was confined to approximately the top 10 mm of the wood sample.

To explore the difference between an air-filled cut and a cut containing a conducting plate, a brass metal plate was placed inside the cut (Figure 14). The measurements were repeated using the same methodology for the E-field parallel and perpendicular measurements.

Figure 14. Metal insert cut for S_{11} measurements.

By repeating the experiment shown in Figure 12a,b, the metal insert produced a change of 7 dB in the S_{11} with respect to air when the E-field was perpendicular to the cut at the cut position (position 0) (see Figure 15a). The brass reflected the electromagnetic field to the antenna. In contrast, for parallel measurements (Figure 15b), the variation in the reflection coefficient S_{11} was less pronounced. At the saw cut position (0 cm), S_{11} was not significantly changed when the cut was filled with air or metal. However, there was a significant change at around −36 dB on the left-hand side of the cut (at points −4, −3) and on the right-hand side of the cut (at point 4). This was due to the wood grain acting as a guide for the reflected field, which was reflected from the brass in both directions.

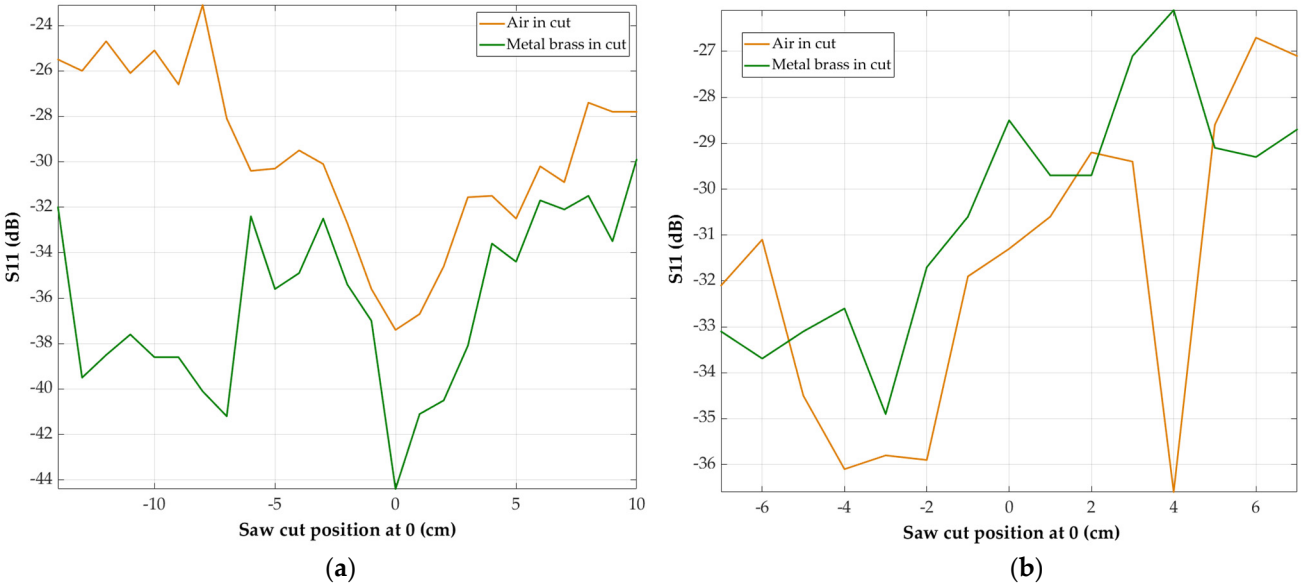

Figure 15. S_{11} measurements for air vs. metal inside the saw cut located at position 0 in water-saturated wood: (**a**) E-field direction was parallel to the wood grain and perpendicular to the cut (reverse side); (**b**) E-field direction was perpendicular to the wood grain and parallel to the cut (reverse side).

4. Discussion

Using a small cavity-backed slot antenna (Figure 1), S_{11} and S_{21} measurements were performed on a kiln-dried pine wood specimen (Figure 2) with the electric field oriented both parallel and perpendicular to the wood grain (Figure 3). The antenna resonated at 4.4 GHz with little variation (<0.01 GHz) observed over the wood length and above natural and artificial anomalies. The S_{11} values (Figure 5) showed a significant anisotropy of 1.5dB, (z score = 3.8, $p < 0.0003$) and S_{21} values (Figure 6) showed significant transmission anisotropy of 22 dB ($p < 0.0003$). The S_{11} parallel measurements above a surface knot in the wood surface (Figures 7 and 8) showed a significant decrease of >5 dB ($p < 0.0003$) accompanied by increases of 5 dB symmetrically located on both sides of the knot. The perpendicular measurements showed a similar variation, but with smaller amplitude.

Two holes were drilled through the wood and S_{11} and S_{21} measurements were made with and without a steel bolt in the hole (Figures 9 and 10). While the changes in S_{11} and S_{21} were not significant when the hole was air-filled, the presence of the bolt created a 2 dB and 4 dB reduction in these parallel measurements, respectively, for a hole 3.5 cm below the measurement surface, and the S_{21} change increased to $>14 \pm 2$ dB (Figure 11).

The effect of a saw cut was investigated for water-saturated and dry wood, and for air and a brass plate in the cut (Figures 12–14). Little effect was observed for the air-filled case with dry wood, but the most significant variation was observed for the parallel S_{11} case in water-saturated wood, which showed a decrease of 8 ± 2 dB. Although the dry wood sample failed to show an effect immediately above the cut, both the air- and brass-filled cuts in water-saturated wood had similar variations immediately above the cut, with an S_{11} variation of $>10 \pm 3$ dB (Figure 15).

5. Conclusions

These results have demonstrated that S11 measurements using a cavity-backed antenna at microwave frequencies can be used to identify imperfections in a pine wood beam. This method is particularly useful for measurements across a large, surface knot, but is also appropriate for an air-filled hole or a steel-filled hole parallel to the measurement surface and the E-field of the antenna. It was established that, for timber with a low moisture content, the detection sensitivity was not particularly strong; however, for high-moisture content wood, a saw cut could be clearly identified.

The cavity-backed slot antenna pressed against the wood surface had significant sensitivity to imperfections in the wood at microwave frequencies, and can be regarded as a simple diagnostic tool to measure the integrity of pine wood beams. It is anticipated that the technique can be readily adapted to all wood types and employed in timber beam processing as a continuous tool for wood integrity measurements. In addition, the technique is suitable for measurements on existing wooden beams in buildings as a rapid scanning tool, providing that one flat surface of the beam is exposed. A significant difference was observed in the S_{11} and S_{21} measurements for the E field perpendicular to the wood grain. The kiln-dried wood had a relatively low conductivity and so the currents generated in the wood by the antenna were relatively weak; consequently, variations in the current direction caused by various imperfections in the wood (knots, holes, bolts, cuts) were not strongly reflected in changes in the two scattering parameters. However, when the conductivity and relatively permittivity were substantially increased by moisture, these parameters were far more sensitive to imperfections.

Author Contributions: Conceptualization, D.V.T.; methodology, investigation, resources measurements, data analysis, M.R.; manuscript preparation, M.R.; manuscript editing, D.V.T. and H.G.E.; project supervision, D.V.T. and H.G.E. All authors have read and agreed to the published version of the manuscript.

Funding: This research received no external funding.

Institutional Review Board Statement: Not applicable.

Informed Consent Statement: Not applicable.

Acknowledgments: M.R. acknowledges the financial support of Griffith University for his PhD scholarship.

Conflicts of Interest: The authors declare no conflict of interest.

References

1. Buchanan, A.; Deam, B.; Fragiacomo, M.; Pampanin, S.; Palermo, A. Multi-Storey Prestressed Timber Buildings in New Zealand. *Struct. Eng. Int.* **2008**, *18*, 166–173. [CrossRef]
2. Kasal, B.; Anthony, R.W. Advances Inin Situ Evaluation of Timber Structures. *Prog. Struct. Engng Mater.* **2004**, *6*, 94–103. [CrossRef]
3. Sørensen, J.D. Framework for Robustness Assessment of Timber Structures. *Eng. Struct.* **2011**, *33*, 3087–3092. [CrossRef]
4. Seim, W.; Hummel, J.; Vogt, T. Earthquake Design of Timber Structures–Remarks on Force-Based Design Procedures for Different Wall Systems. *Eng. Struct.* **2014**, *76*, 124–137. [CrossRef]
5. Frühwald Hansson, E. Analysis of Structural Failures in Timber Structures: Typical Causes for Failure and Failure Modes. *Eng. Struct.* **2011**, *33*, 2978–2982. [CrossRef]
6. Cruz, H.; Yeomans, D.; Tsakanika, E.; Macchioni, N.; Jorissen, A.; Touza, M.; Mannucci, M.; Lourenço, P.B. Guidelines for On-Site Assessment of Historic Timber Structures. *Int. J. Archit. Herit.* **2015**, *9*, 277–289. [CrossRef]
7. Balasso, M.; Hunt, M.; Jacobs, A.; O'Reilly-Wapstra, J. Development of non-destructive-testing based selection and grading strategies for plantation Eucalyptus Nitens sawn boards. *Forests* **2021**, *12*, 343. [CrossRef]
8. Ito, N.; Okubo, N.; Kurata, Y. Nondestructive near-infrared spectroscopic analysis of oils on wood surfaces. *Forests* **2019**, *10*, 64. [CrossRef]
9. Ida, N.; Meyendorf, N. (Eds.) *Handbook of Advanced Nondestructive Evaluation*; Springer International Publishing: Cham, Switzerland, 2019; ISBN 978-3-319-26552-0.
10. Huan, Z.; Jiao, Z.; Li, G.; Wu, X. Velocity error correction based tomographic imaging for stress wave nondestructive evaluation of wood. *BioResources* **2018**, *13*, 2530–2545. [CrossRef]
11. Liang, S.; Fu, F. Strength loss and hazard assessment of Euphrates poplar using stress wave tomography. *Wood Fiber Sci.* **2012**, *44*, 54–62.
12. Ramasamy, S.; Moghtaderi, B. Dielectric Properties of Typical Australian Wood-Based Biomass Materials at Microwave Frequency. *Energy Fuels* **2010**, *24*, 4534–4548. [CrossRef]
13. Olmi, R.; Bini, M.; Ignesti, A.; Riminesi, C. Dielectric Properties of Wood from 2 to 3 GHz. *J. Microw. Power Electromagn. Energy* **2000**, *35*, 135–143. [CrossRef] [PubMed]
14. Olmi, R.; Bini, M.; Ignesti, A.; Riminesi, C. Non-Destructive Permittivity Measurement of Solid Materials. *Meas. Sci. Technol.* **2000**, *11*, 1623–1629. [CrossRef]
15. Ulaby, F.T.; Ravaioli, U. *Fundamentals of Applied Electromagnetics*, 7th ed.; Pearson: Boston, MA, USA, 2015; ISBN 978-0-13-335681-6.
16. Gholizadeh, S. A Review of Non-Destructive Testing Methods of Composite Materials. *Procedia Struct. Integr.* **2016**, *1*, 50–57. [CrossRef]
17. Nadakuduti, J.; Chen, G.; Zoughi, R. Semiempirical Electromagnetic Modeling of Crack Detection and Sizing in Cement-Based Materials Using Near-Field Microwave Methods. *IEEE Trans. Instrum. Meas.* **2006**, *55*, 588–597. [CrossRef]
18. Camuffo, D. Standardization Activity in the Evaluation of Moisture Content. *J. Cult. Herit.* **2018**, *31*, S10–S14. [CrossRef]
19. Emelyanenko, A.A.; Doh, J.-H.; Espinosa, H.G.; Thiel, D.V. Microwave Measurements in Cured Concrete—Experiment and Modelling. In Proceedings of the 2018 Australian Microwave Symposium (AMS), Brsibane, Australia, 6–7 February 2018; pp. 67–68.
20. Fratticcioli, E.; Dionigi, M.; Sorrentino, R. A Simple and Low-Cost Measurement System for the Complex Permittivity Characterization of Materials. *IEEE Trans. Instrum. Meas.* **2004**, *53*, 1071–1077. [CrossRef]
21. Available online: https://qtimber.daf.qld.gov.au/timber-factsheet/pine%2C%20radiata (accessed on 10 October 2021).